Relaxation Dynamics in Glycerol−Water Mixtures. 2. Mesoscopic Feature in Water Rich Mixtures

Yoshihito Hayashi, Alexander Puzenko, Igal Balin, Yaroslav E. Ryabov,† and Yuri Feldman*

Department of Applied Physics, The Hebrew University of Jerusalem, Givat Ram, 91904, Jerusalem, Israel

Received: January 25, 2005; In Final Form: March 7, 2005

The relaxation dynamics of water-rich glycerol−water mixtures is studied by broadband dielectric spectroscopy (BDS) at 173−323 K and differential scanning calorimetry (DSC) at 138−313 K. These data indicate the existence of the critical concentration of 40 mol % glycerol. In the studied temperature range for water-rich glycerol mixtures, the two states of water (ice and interfacial water) are observed in addition to water in the mesoscopic 40 mol % glycerol−water domains. The possible kinetics of water exchange between different water states is discussed in order to explain the mechanism of the broad melting behavior observed by DSC.

Introduction

The study of slow dynamics in glass forming liquids is currently a significant challenge in the research field of soft condensed matter science.[1−6] Hydrogen bonding (H-bonding) liquids and their mixtures occupy a special place among complex systems due to the existence of directed H-bonds. In contrast to covalent bonds, the H-bonds can be rearranged relatively easily. Although an enormous amount of literature exists which relates to the investigation of H-bonding systems, there is still a lack of clear understanding even on the level of dynamics in "simple" water or alcohols. Among them, glycerol[3,7−9] and its mixtures with water[10] are widely used as excellent models to study the cooperative dynamics. In the previous paper (part 1 of this series),[11] we reported a broadband dielectric spectroscopy (BDS) study of glycerol−water mixtures in the glycerol-rich region, and discussed the mechanism of dc-conductivity, the main relaxation process and the excess wing in terms of so-called master plots. The master plots were obtained by a simple normalization where the imaginary part data (dielectric loss) of the complex permittivity was normalized by its maximum value ϵ''_{max} and the result was presented versus the dimensionless variable f/f_{max} where f_{max} corresponds to the frequency of the maximum loss. Figure 1 shows typical master plots of 32 spectra at different temperatures. All normalized spectra traced with the same single curve through dc-conductivity, the main relaxation process, and the excess wing. This result indicates that the dielectric response at both high and low frequencies follows the same temperature dependence of the main relaxation process and leads to the hypotheses that the relaxation mechanism of the excess wing, the main process and dc-conductivity are based on the same origin.

Such universal dielectric behavior disappeared at higher water concentrations (lower than 60 mol % of glycerol) due to the appearance of water−water interactions coexisting with the glycerol−glycerol and glycerol−water interactions. The water−water interactions were also discussed recently by Sudo et al. in view of water and glycerol cooperative domains.[10] Therefore, we can assume that H-bond networks in water-rich mixtures are not homogeneous on a mesoscopic level, although the detailed features of such heterogeneous structures are not fully known. With increasing amounts of water, the water pools grow in size, which leads to their freezing at low temperatures. In the case of H-bonding liquid mixtures, however, dynamical and structural properties in frozen states have not yet been extensively studied. In the present paper, we report BDS and differential scanning calorimetry (DSC) measurements of a glycerol−water mixture at a high water concentration range and temperature intervals including water-frozen state.

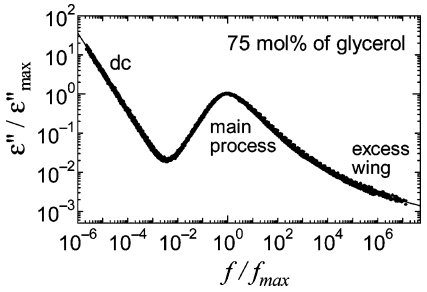

Figure 1. Master plot of the imaginary part of the dielectric spectra for 75 mol % of glycerol in which 32 spectra at temperatures from 197 to 290 K were normalized and shown.

Materials and Methods

As it was described in our previous paper,[11] the glycerol−water mixtures with alcohol content between 5 and 95 mol % and with intervals of 5 mol % were prepared from anhydrous glycerol (product number 49767, Fluka, Buchs, Switzerland) and double distilled water (resistivity 18 MΩ cm).

BDS measurements were performed in the frequency range from 1 Hz to 250 MHz at temperatures from 173 to 323 K (for 5−95 mol % of glycerol) and from 175 to 292 K (for 100 mol % of glycerol) at intervals of 3 K by using a Novocontrol BDS-80. All of the measurements were performed after temperature stabilization starting from the lowest temperatures to higher temperatures, consecutively. BDS data of glycerol-rich mixtures are partly reported in our previous paper.[11]

DSC measurements of glycerol-water mixtures (80, 60, 40, 30, 20, 15, 10, and 2.5 mol % of glycerol) were performed by

* To whom correspondence should be addressed. E-mail: yurif@vms.huji.ac.il. Phone: +972 2 6586187. Fax: +972 2 5663878.

† Present address: Department of Chemistry & Biochemistry, Center of Biomolecular Structure & Organization, University of Maryland, College Park, MD 20742.

10.1021/jp050425d CCC: $30.25
Published on Web 04/07/2005

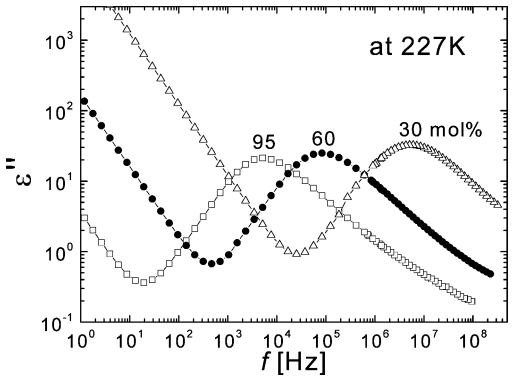

Figure 2. Typical dielectric spectra of glycerol-water mixtures at 227 K for 95 (open box), 60 (full circle), and 30 (open triangle) mol % of glycerol. The accuracy of dielectric data is better than 3%.[3]

use of a DSC 2920 calorimeter (TA Instruments) in the temperature interval from 138 to 313 K (173−313 K for 20 mol %) with a heating rate of 10 K/min.

Results and Discussion

Figure 2 shows the typical isothermal behavior of dielectric losses of glycerol−water mixtures. Let us consider the dynamics of glycerol−water mixtures in terms of the characteristic time $\tau_{max} = 1/(2\pi f_{max})$ temperature dependences of the main relaxation process. In the glycerol-rich region (100−40 mol %), as mentioned in the previous paper[11] and as shown in Figure 3a, τ_{max} is well described by the Vogel−Fulcher−Tammann (VFT) law[12−14] with the same value of fragility ($D = 22.7$) and almost the same values of pre-exponent factor ($\ln\tau_\upsilon = -35.9$ to -36.4) as follows:

$$\tau_{max} = \tau_v \exp\{DT_v/(T - T_v)\} \quad (1)$$

where T_v is the Vogel-Fulcher temperature. The plots in Figure 3a represent the experimental data, for glycerol−water mixtures, where the glycerol concentration is systematically changed with the steps of 5 mol %, and the solid lines show the fitting results according to the VFT law. The results indicate that the relaxation mechanisms and H-bond networks for the glycerol-rich mixtures are similar to those of pure glycerol.

Below 40 mol % of glycerol and at lower temperatures (below ~230 K), the τ_{max} can be describe by the Arrhenius law as shown in Figure 3a (dashed lines), although it was continuously changed to the VFT temperature behavior at higher temperatures. Our analyses and comparison with the literature[10] shows that τ_{max} temperature behavior in water-rich regions can depend on temperature history, although no differences were found in glycerol-rich regions above T_g (here T_g is the glass transition temperature). These results may indicate that mesoscopic structures of H-bond networks in the glycerol-rich regions are homogeneous. In contrast, in the water-rich regions, such mixtures have a more complicated dynamic behavior. Glycerol molecules cannot provide all water molecules with H-bond networks, and correspondingly, the system forms so-called glycerol and water cooperative domains, respectively. Dynamic structures of such domains can depend on temperature hysteresis. The critical molar fraction (x_g) would relate to the numbers of H-bonds of glycerol ($n_g \approx 6$; reported in ref 15) and water ($n_w = 4$) molecules, thus: $x_g = 100\% n_w/(n_w + n_g) = 40\%$.

The existence of this critical concentration of 40 mol % of glycerol is well supported by the results obtained from further study of the water-rich region. Figure 3b shows the temperature dependence of τ_{max} for 20 mol % of glycerol. At lower

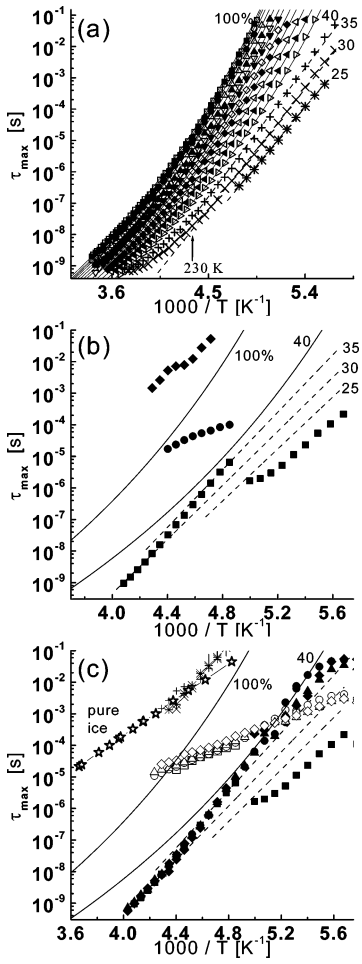

Figure 3. (a) Temperature dependencies of τ_{max} for the main relaxation process of glycerol-water mixtures in 100 to 25 mol %. (b) Temperature dependencies of τ_{max} for 20 mol % (full box: main relaxation process, full diamond: relaxation process due to ice, and full circle: relaxation process due to interfacial water). The solid curves are the same as the curves shown in (a) for 100 and 40 mol % as well as the dashed lines for 35, 30, and 25 mol %. (c) Temperature dependencies of τ_{max} for water-rich mixtures. The full and open symbols show the main relaxation process and the relaxation process due to interfacial water, respectively (box: 20, circle: 15, triangle: 10, and diamond 5 mol %). Temperature dependencies of τ_{max} for the relaxation process due to ice also shown (plus: 20, cross: 15, asterisk: 10, and vertical bar: 5 mol %), and the open stars show the experimental results for bulk ice.[16]

temperatures, τ_{max} demonstrates a behavior similar to that of higher glycerol concentrations. However, when the temperature was increased and approached $T = 206$ K, a crystallization of the extra water occurred and τ_{max} increased up to nearly the same values as that of 35 mol % of glycerol. After the crystallization, two additional Arrhenius type relaxation processes were observed (Figure 4 shows typical dielectric spectra of before and after the crystallization). One of these relaxation processes is due to the presence of ice cores since the relaxation time and its activation energy (~77 kJ/mol) is similar to the well-known values for the bulk ice which were reported by Auty and Cole[16] (Figure 3c). Another relaxation process may relate to the presence of some interfacial water between the ice core and mesoscopic glycerol−water domain. The glycerol concentration of this domain was enriched up to the critical concentration ~40 mol % by the freezing of the extra water that was free from the glycerol H-bond networks.

In the cases of 15, 10, and 5 mol % of glycerol−water mixtures, the ice cores have already been formed during the

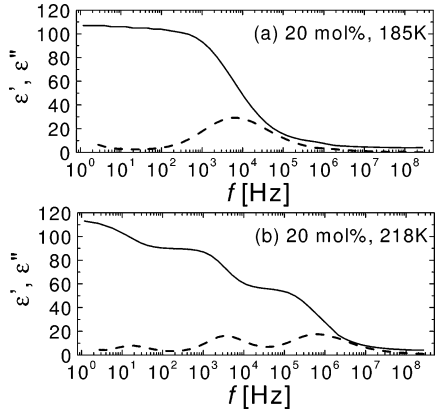

Figure 4. Typical dielectric spectra of 20 mol % of glycerol-water mixtures at (a) 185 K (supercooled state) and (b) 218 K (frozen state), where solid and dashed curves show the real and imaginary part of complex dielectric permittivity. Each relaxation process in the frozen state was fitted by the modified Cole−Davidson function proposed in the previous paper,[11] Cole−Cole and Debye relaxation functions, respectively, to separate the main process, the process due to interfacial water, and the process due to ice. Note that contribution caused by dc-conductivity was subtracted from the dielectric loss curve and shown in (b).

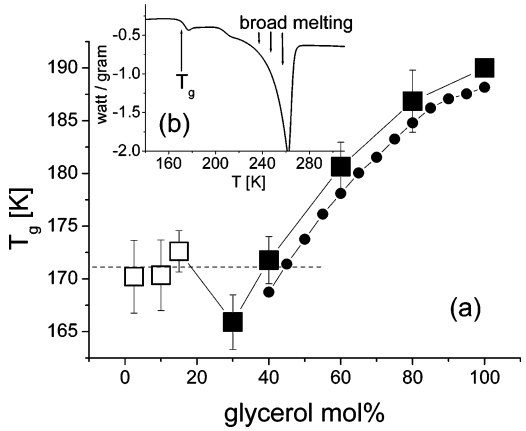

Figure 5. (a) Glycerol concentration dependence of the glass-transition temperature obtained by DSC measurements (full box: supercooled or liquid sate, and open box: frozen state) and by BDS data (full circle). The DSC data point for 100% glycerol is taken from a previous work.[6] (b) Typical raw data of DSC measurements (10 mol % of glycerol), where the glass transition and a broad melting behavior were observed.

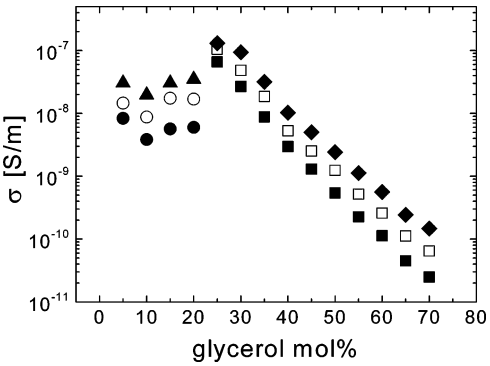

Figure 6. Glycerol concentration dependencies of dc-conductivity (full box: liquid or supercooled state at 209 K, full circle: frozen state at 209 K, open box: liquid or supercooled state at 212 K, open circle: frozen state at 212 K, full diamond: liquid or supercooled state at 215 K, and full triangle: frozen state at 215 K).

quenching down to the starting temperature of the BDS measurements and τ_{max} of the main relaxation process for all these mixtures shows values that are similar to those of 35 or 40 mol % of the glycerol−water mixtures (see Figure 3c). Furthermore, the two additional relaxation processes (due to ice core and interfacial water) also traced the same lines, respectively. It is worth noting that the activation energy of ∼33 kJ/mol of the relaxation process resulting from interfacial water is similar to the reported values ∼28 kJ/mol for bound water on protein-surface in aqueous solutions[17] and ∼30−40 kJ/mol for surface water on porous glasses, depending on the porous glass preparation.[18] The relaxation time for this interfacial water is ∼100 times larger than that for the bound water reported in protein solutions.[17] In the case of bound water in protein solution, this interfacial water is surrounded by other fast-mobile water molecules from the solvent. In the case of water-rich glycerol−water mixtures, the interfacial water molecules would be confined between two slow regions such as the ice and glycerol−water domains, therefore, mobility of the interfacial water in water−glycerol mixtures would be highly restricted.

Note that Maxwell−Wagner surface polarization[19] may partly contribute in the same frequency range as the relaxation process due to the ice cores. However, estimation of its contribution, as well as exact calculation of the correct dielectric strength due to the ice structure is problematic because of uncertainties, both in the radius of the ice cores and in the exact value of conductivity of the interfacial water.

The glass transition temperature (T_g), which is defined as a temperature where the relaxation time is 100 s,[20,21] was evaluated for glycerol-water mixtures using temperature dependencies of τ_{max} for the main dielectric relaxation process (see Figure 3a). As shown in Figure 5a, the glass transition temperatures (T_g) obtained by DSC measurements were in good agreement with BDS data. It is worth pointing out that T_g for 2.5, 10, and 15 mol % of glycerol−water mixtures in the frozen state all have the values close to the T_g for 40 mol % of the glycerol−water mixture. This result indicates that the glass transition observed in the frozen state results from the mesoscopic glycerol−water domains of 40 mol % glycerol.

Moreover, even simple dc-conductivity data obtained by BDS at particular temperatures show concentration independent behaviors in the frozen state, and the values are close to that of 40 or 35 mol % of glycerol (Figure 6). Note that these results support the hypothesis that the mechanism of dc-conductivity at low temperatures is most likely H-bond defect translocation as discussed in the previous paper,[11] because the increase of ionic impurities with water concentration did not affect the frozen state as shown in Figure 6.

To estimate the ratio between the amounts of water in the mesoscopic glycerol−water domains, interfacial water and ice core in glycerol−water mixtures, one can use the melting-enthalpy ΔH obtained from DSC data. Note that in this specific case, the total melting-enthalpy (ΔH) was obtained by integration of the transition heat capacity (ΔC_P) over the broad melting temperature interval

$$\Delta H = \int_{T_1}^{T_2} \Delta C_P \, dT = \int_{T_1}^{T_2} (C_P - C_{P(baseline)})_p \, dT \quad (2)$$

where T_1 is the starting temperature of the broad melting (223 K for 10 mol % glycerol, see Figure 5b), T_2 is the temperature of the phase transition, and $C_{P(baseline)}$ is the extrapolated heat capacitance baseline in the same temperature interval.[22] Thus, amount of ice below the starting temperature of the broad melting was estimated by the ratio ($\Delta H/\Delta H_0$) where ΔH_0 is the melting-enthalpy of bulk ice.[23] Using the known total amount of water and the critical 40 mol % concentration, we can

estimate that in 10 mol % of glycerol-water mixture, for example, we have approximately 44 mol % of ice, 15 mol % of water in the mesoscopic domains, and 31 mol % of interfacial water. This estimation using DSC data also shows the presence of a significant amount of interfacial water in the frozen state of the glycerol−water mixtures.

According to this fact, the existence of three water states: water in glycerol H-bond networks ($H_2O_{(GW)}$), water in ice structure ($H_2O_{(ice)}$) and the interfacial water ($H_2O_{(interface)}$) can be considered. Let us discuss a possible kinetic mechanism of the broad melting behavior. The relations between the three states of water can be described by

$$H_2O_{(GW)} \underset{k_2}{\overset{k_1}{\rightleftharpoons}} H_2O_{(interface)} \underset{k_4}{\overset{k_3}{\rightleftharpoons}} H_2O_{(ice)} \tag{3}$$

where k_1, k_2, k_3, and k_4 are the exchanges rates (e.g., the exchange velocity from $H_2O_{(GW)}$ to $H_2O_{(interface)}$ is described by $v_1 = k_1\,[H_2O_{(GW)}]$, where $[H_2O_{(GW)}]$ is the mole concentration of $H_2O_{(GW)}$). If the system is in an equilibrium state, apparently $[H_2O_{(interface)}]$ does not change. Therefore, it can be described as $k_1[H_2O_{(GW)}] + k_4[H_2O_{(ice)}] = (k_2 + k_3)[H_2O_{(interface)}]$. Let us consider one particular concentration of the glycerol−water mixture in the water-rich region. Due to the critical concentration of the 40 mol %, it is reasonable to assume that $[H_2O_{(GW)}]$ is not dependent on temperature, and it is clear that the total mole concentration of water (C_{total}) is constant. Therefore, the concentration of $H_2O_{(interface)}$ can be described by $[H_2O_{(interface)}] = C_W - [H_2O_{(ice)}]$, where $C_W = C_{total} - [H_2O_{GW}]$ is also a constant. Thus, one can obtain

$$[H_2O_{(interface)}] = \frac{k_1[H_2O_{(GW)}] + k_4 C_W}{k_2 + k_3 + k_4} \tag{4}$$

It is reasonable to assume $k_1 \cong k_2$ because the water exchange in both directions between $H_2O_{(GW)}$ and $H_2O_{(interface)}$ are caused by the same rearrangement of mesoscopic structures of H-bond networks of the glycerol−water mixture. In other words, both k_1 and k_2 are related to the relaxation time of the mesoscopic glycerol−water domain. Furthermore, it is clear that the probability of a water molecule to return back to the interface from the ice core is much smaller than in the reverse direction and hence $k_3 \gg k_4$. Thus, finally we can obtain

$$[H_2O_{(interface)}] \cong \frac{\frac{k_2}{k_3}[H_2O_{(GW)}]}{1 + \frac{k_2}{k_3}} \cong \frac{C\frac{k_2}{k_3}}{1 + \frac{k_2}{k_3}} \tag{5}$$

where C is a constant. Taking into account that the total water amount is a constant value, the relation (5) shows that any increase of the ratio k_2/k_3 leads to a decrease of ice core and an increase of $H_2O_{(interface)}$. It clarifies the broad melting behavior of the glycerol−water mixture observed by DSC measurements (e.g., Figure 5b) and explains why τ_{max} does not follow the 40 mol % curve at higher temperatures (Figure 3c). In this temperature region, a faster replacement between $H_2O_{(GW)}$ and $H_2O_{(interface)}$ allows the mixture to retain more water in the liquid phase than the expected amount based on the critical concentration of 40 mol %. Some part of the extra-interfacial water can penetrate the mesoscopic glycerol−water domain and can affect the dynamic properties of this domain. Nevertheless, the same number of the penetrated water molecules should be classified as $H_2O_{(interface)}$ by relations (3)−(5), because it is this number of water molecules that are free from the glycerol H-bond network in the mesoscopic domain.

Acknowledgment. The authors thank Prof. Udo Kaatze (Georg-August-Universitaet, Germany) and Prof. Ilyin Valery (the Weizmann Institute of Science, Israel) for helpful discussion.

References and Notes

(1) Mishima, O.; Stanley, H. E. *Nature (London)* **1998**, *396*, 329.
(2) Donth, E. *The Glass Transition: Relaxation Dynamics in Liquids and Disordered Materials*; Springer-Verlag: Berlin, 2001.
(3) Kremer, F.; Schönhals, A. *Broadband Dielectric Spectroscopy*; Springer-Verlag: Berlin, 2003.
(4) Ngai, K. L.; Rendell, R. W.; Plazek, D. J. *J. Chem. Phys.* **1991**, *94*, 3018.
(5) Angell, C. A.; Ngai, K. L.; McKenna, G. B.; McMillan, P. F.; Martin, S. W. *J. Appl. Phys.* **2000**, *88*, 3113.
(6) Ryabov, Ya. E.; Hayashi, Y.; Gutina, A.; Feldman, Y. *Phys. Rev. B* **2003**, *67*, 132202.
(7) Angell, C. A. *J. Non-Cryst. Solids* **1991**, *131−133*, 13.
(8) Lunkenheimer, P.; Pimenov, A.; Dressel, M.; Goncharov, Yu. G.; Böhmer, R.; Loidl, A. *Phys. Rev. Lett.* **1996**, *77*, 318.
(9) Johari, G. P.; Whalley, E. *Faraday Symp. Chem. Soc.* **1972**, *6*, 23.
(10) Sudo, S.; Shimomura, M.; Shinyashiki, N.; Yagihara, S.; *J. Non-Cryst. Solids* **2002**, *307−310*, 356 (with personal communication about the protocol of temperature controlling).
(11) Puzenko, A.; Hayashi, Y.; Ryabov, Ya. E.; Balin, I.; Feldman, Yu.; Kaatze, U.; Behrends, R. *J. Phys. Chem. B* **2005**, *109*, 6031.
(12) Vogel, H. *Phys. Z.* **1921**, *22*, 645.
(13) Fulcher, G. S. *J. Am. Ceram. Soc.* **1925**, *8*, 339.
(14) Tammann, G.; Hesse, W. *Z. Anorg. Allg. Chem.* **1926**, *156*, 245.
(15) Padró, J. A.; Saiz, L.; Guàrdia, E. *J. Mol. Struct.* **1997**, *416*, 243.
(16) Auty, R. P.; Cole, R. H. *J. Chem. Phys.* **1952**, *20*, 1309.
(17) Miura, N.; Hayashi, Y.; Shinyashiki, N.; Mashimo, S. *Biopolymers* **1995**, *36*, 9.
(18) Gutina, A.; Antropova, T.; Rysiakiewicz-Pasek, E.; Virnik, K.; Feldman, Yu. *Microporous Mesoporous Mater.* **2003**, *58*, 237.
(19) Takashima, S. *Electrical Properties of Biopolymers and Membranes*; IOP Publishing: Philadelphia, 1989.
(20) Böhmer, R.; Ngai, K. L.; Angell, C. A.; Plazek, D. J. *J. Chem. Phys.* **1993**, *99*, 4201.
(21) Hayashi, Y.; Miura, N.; Shinyashiki, N.; Yagihara, S.; Mashimo, S.; *Biopolymers* **2000**, *54*, 388.
(22) Pathria, R. K.; *Statistical Mechanics*; Butterworth-Heineman: Oxford, U.K., 1996; p. 15.
(23) Naoi, S.; Hatakeyama, T.; Hatakeyama, H. *J. Therm. Anal. Calorim.* **2002**, *70*, 841.